

NMR studies of hydrogen motion in nanostructured hydrogen–graphite systems

G. Majer^{a,*}, E. Stanik^a, S. Orimo^b

^aMax-Planck-Institut für Metallforschung, Heisenbergstr. 3, Stuttgart, 70569 Germany

^bHiroshima University, Faculty of Integrated Arts and Sciences, Higashi-Hiroshima 739-8521, Japan

Received 4 July 2002; accepted 17 October 2002

Abstract

Nanostructured hydrogen–graphite systems, $C^{\text{nano}}H_x$ ($x = 0.24, 0.31, 0.96$), have been characterized by first nuclear magnetic resonance (NMR) measurements. The NMR spectrum of $C^{\text{nano}}H_{0.96}$ is well represented by the sum of a Lorentzian and a Gaussian line, indicating two types of hydrogen coordinations. These two components may be ascribed to hydrogen in graphite interlayers and hydrogen chemisorbed at dangling bonds. Information on the hydrogen hopping frequencies is provided by the spin–lattice relaxation rate T_1 . The temperature dependence of T_1 yields high hydrogen diffusivities and low activation energies of $E_a \approx 0.1$ eV. A change in the T_1 data of $C^{\text{nano}}H_x$ with $x = 0.24$ and 0.31 occurred after the samples had been heated to about 400–430 K. This suggests that in this temperature range hydrogen atoms start to occupy sites with different site energies, resulting in a distribution of the activation energies for hydrogen motion.

© 2003 Elsevier B.V. All rights reserved.

Keywords: Nanostructured graphite; NMR; Spin–lattice relaxation; H motion

1. Introduction

Nanostructured materials are becoming increasingly important from the viewpoint of applications as well as for basic research. Owing to the rather large volume fraction of grain boundaries many physical properties are fundamentally changed in samples with crystalline grains in the nanometer range. Recent nuclear magnetic resonance (NMR) measurements of hydrogen in nanostructured vanadium–hydrogen systems, for example, revealed pronounced differences in the hydrogen dynamics inside the grains and in the intergrain regions [1]. For hydrogen storage and energy conversion types of applications carbon-related nanostructured systems are especially interesting [2] because carbon is a lightweight and inexpensive material.

A simple but reliable method to prepare nanostructured hydrogen–graphite systems, $C^{\text{nano}}H_x$, is mechanical mil-

ling of graphite under hydrogen atmosphere. Several samples obtained after different milling times were systematically investigated to obtain fundamental information about the structures, hydrogen concentrations, and hydrogen desorption properties [3,4]. The hydrogen concentration reaches 7.4 wt.% ($C^{\text{nano}}H_{0.96}$) after milling for 80 h. Two desorption peaks of hydrogen, starting at about 600 K and 950 K, respectively, are observed in thermal desorption mass spectroscopy [4]. About 80% of the total hydrogen content desorbs at the first desorption peak. The second desorption peak is induced by recrystallization of the nanostructured graphite. The same desorption phenomena are observed in samples mechanically milled under deuterium atmosphere [4]. This confirms that the hydrogen (deuterium) has been stored inside the nanostructured graphite, and is not due to adsorbed water or other hydrogen sources. Similar studies of the hydriding and desorption properties have been performed recently on nanostructured boron nitride [5].

The present work reports on preliminary NMR measurements of hydrogen in $C^{\text{nano}}H_x$ ($x = 0.24, 0.31, 0.96$). The main goals were to investigate the local environments and the dynamical processes of hydrogen in $C^{\text{nano}}H_x$.

*Corresponding author. Tel.: +49-711-689-1821.

E-mail address: majer@nmr.mpi-stuttgart.mpg.de (G. Majer).

2. Experimental details

The samples of the present work ($C^{\text{nano}}H_x$ with $x = 0.24, 0.31$ and 0.96) were prepared by ball milling of graphite under hydrogen atmosphere as described in [3,4]. The material of the vials and the balls was selected carefully to minimize the amount of elemental iron introduced into the sample during the mechanical milling, since magnetic impurities may have a severe effect on the NMR data [6]. The samples with $x = 0.24$ and 0.96 were prepared by ball milling with chromium-steel balls and vials under an initial hydrogen pressure of 1.0 MPa for 5 and 80 h, respectively. In order to investigate the possible effect of magnetic impurities, a third $C^{\text{nano}}H_x$ sample was prepared by using agate vials and balls. Owing to the smaller mass and thus the lower impact of the agate balls, longer milling times were required in this case. This sample was ball milled for 200 h with an initial hydrogen pressure of 0.3 MPa. After 80 h and after 160 h of milling, further hydrogen of 0.3 MPa was introduced into the vial. The hydrogen content of the sample thus obtained is $x = 0.31$. All samples were handled in an argon-filled glove box before and after milling to minimize oxidation and water adsorption. For the NMR measurements the samples were sealed in glass tubes of an outer diameter of 5 mm and a length of 20 mm.

The NMR measurements were performed with a home-built Fourier transform spectrometer using phase-alternating pulse schemes and quadrature detection. The sample temperature was maintained within about ± 0.2 K by means of a digital PID controller combined with ohmic heating, and it was monitored independently by two calibrated platinum resistors. Temperatures below room temperature were achieved by cooling with liquid nitrogen in a separate cryostat in the room-temperature bore of the superconducting magnet. The proton spin–lattice relaxation rates T_1 were determined using an inversion-recovery pulse sequence ($180^\circ - \tau_1 - 90^\circ$) with different waiting times τ_1 . The recovered magnetization was inspected by measuring the free induction decay following the 90° pulse after the ring-down time of the NMR probe ($\tau_{\text{delay}} \approx 10 - 15 \mu\text{s}$). The T_1 measurements were performed at a resonance frequency of 67.7 MHz in a temperature range from 145 K to 430 K.

3. Results and discussion

The first proton NMR spectrum measured on $C^{\text{nano}}H_{0.96}$ at room temperature is shown in Fig. 1. The spectrum is well represented by the sum of a Lorentzian and a Gaussian line, indicating two types of hydrogen coordinations. The Gaussian line has a full width at half maximum of about $\Delta\nu_{\text{Gauss}} = 46$ kHz, whereas the Lorentzian line is only about $\Delta\nu_{\text{Lorentz}} = 4.5$ kHz wide. These results suggest different hydrogen mobilities, resulting in motional nar-

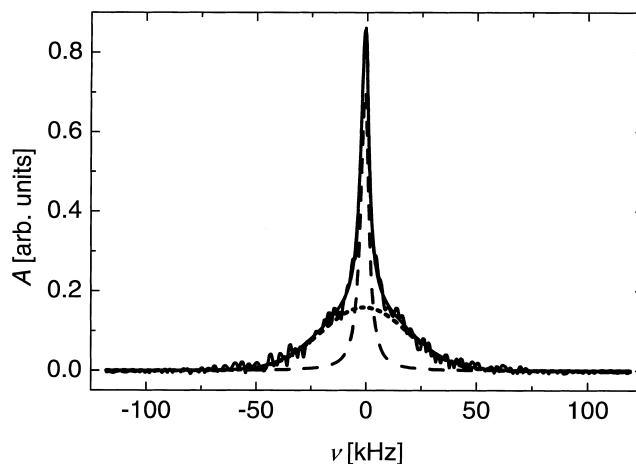


Fig. 1. Proton NMR spectrum of $C^{\text{nano}}H_{0.96}$ obtained by Fourier transformation of the free induction decay (FID) following a 90° r.f.-pulse. The smooth solid curve on top of the measured spectrum is obtained by fitting the sum of a Gaussian curve (short dashes) and a Lorentzian curve (long dashes) to the data.

rowing of the NMR signal related to the more mobile fraction. However, other interpretations cannot yet be completely ruled out. The radial distribution function spectrum obtained by neutron diffraction measurements on nanostructured graphite–deuterium-systems reveals also two types of deuterium coordinations, one with a C–D distance of about 0.11 nm and one with a broader distribution of C–D distances around 0.18 nm [3,7]. The latter corresponds to deuterium atoms physisorbed in the graphite interlayers. The binding energy of the van der Waals interaction responsible for physisorption is of the order of about 0.1 eV, resulting in a comparatively high hydrogen (deuterium) mobility. The C–D distance of 0.1 nm corresponds to covalent C–D bonds with significantly higher binding energies [3]. From these results we may conclude that the narrow NMR line in $C^{\text{nano}}H_{0.96}$ is due to hydrogen atoms physisorbed in the graphite interlayers and the broader line corresponds to hydrogen chemisorbed at defect structures forming covalent C–H bonds.

The relative numbers of hydrogen atoms in the two components are roughly given by the relative intensities of the narrow and broad NMR lines. In $C^{\text{nano}}H_{0.96}$ the intensity of the broad NMR line is about 1.8 times that of the narrow line, and this fraction seems to increase with increasing milling time. However, for a more precise quantitative analysis one has to take into account that the NMR signal is already reduced when the data acquisition starts after the ring-down time of the NMR probe. The decay of the nuclear magnetization with time is not exactly known for $t \leq \tau_{\text{delay}}$, and the two components, which contribute to the NMR signal, decay differently. This introduces an uncertainty in the data analysis but, as long as the assumptions about the magnetization decay were reasonable, it was always found that more hydrogen atoms contribute to the broad NMR line than to the narrow one.

This is consistent with neutron diffraction measurements on $C^{\text{nano}}D_{0.661}$ [7] and, thus, it further supports the assignment of the broad and narrow NMR lines to chemisorbed and physisorbed hydrogen atoms. By comparing the areas of the peaks at 0.18 nm and 0.1 nm, the neutron data indicate that about 40% of the absorbed deuterium atoms are located in the graphite interlayers and about 60% form covalent C–D bonds [7].

In order to study the hydrogen mobility in $C^{\text{nano}}H_x$, measurements of the hydrogen spin–lattice relaxation rate Γ_1 were performed. For all three samples, the magnetization observed after an inversion-recovery pulse sequence could be reasonably well described by a single-exponential recovery curve. It was not possible to determine different Γ_1 values for the broad and narrow NMR lines. An attempt to integrate only over the frequency range of the broad line yielded similar Γ_1 values but with significantly higher experimental uncertainties. This may indicate that an exchange of hydrogen atoms between the two components occurs on the time scale of the Γ_1 measurements. Fig. 2

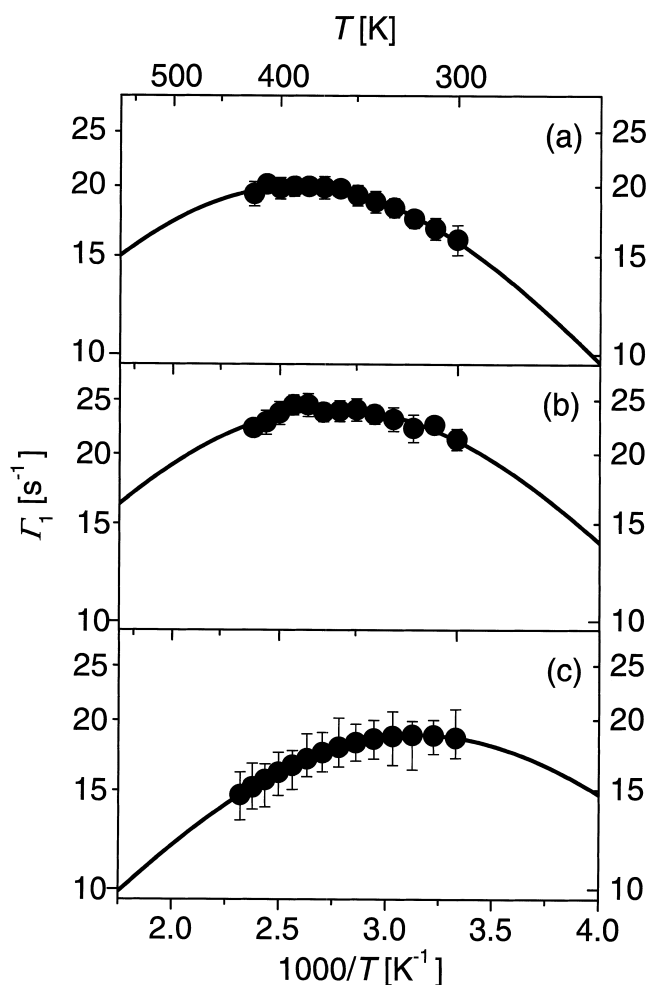


Fig. 2. First measurements of the spin–lattice relaxation rate Γ_1 of hydrogen in nanostructured hydrogen–graphite systems (a) $C^{\text{nano}}H_{0.96}$, (b) $C^{\text{nano}}H_{0.31}$, and (c) $C^{\text{nano}}H_{0.24}$. The data were taken at 67.7 MHz. The solid lines represent BPP curves with activation energies of about 0.1 eV.

shows the Γ_1 data measured on $C^{\text{nano}}H_x$ ($x = 0.24, 0.31, 0.96$) in a first run from room temperature to about 430 K. The spin–lattice relaxation due to the dipole–dipole interaction between the protons is usually described by the BPP model [6]

$$\Gamma_{1,\text{dip}} = \frac{4}{3} \frac{M_2}{\omega_0} \left[\frac{y}{4 + y^2} + \frac{y}{1 + y^2} \right], \quad (1)$$

with $y = \omega_0 \tau_d$ where $\omega_0/2\pi$ denotes the NMR frequency and τ_d is the mean dwell time of the migrating hydrogen atoms. M_2 is the so-called second moment of the dipole–dipole interaction, which determines the relaxation strength. The solid lines in Fig. 2 are obtained by fitting Eq. (1) to the data under the assumption of a single thermally activated process of hydrogen motion according to

$$\tau_d = \tau_0 \exp(E_a/k_B T). \quad (2)$$

The activation energies for hydrogen motion corresponding to these fitting curves are $E_a = 82, 87$ and 89 meV for $x = 0.96, 0.31$ and 0.24 , respectively. Within the uncertainties of the fitting parameters, which are rather high due to the limited temperature ranges covered by these data, the E_a values of all three samples agree. They are all of the order of 0.1 eV, independent of the hydrogen content of the sample. An activation energy of $E_a \approx 0.1$ eV corresponds well to the van der Waals binding energy of hydrogen to a graphene sheet, indicating that the dipolar relaxation is determined by the hydrogen diffusion in the graphite interlayers. The maximum of $\Gamma_{1,\text{dip}}$ occurs at a position at which the hydrogen hopping frequency is very close to the NMR frequency. The BPP model gives $\tau_d = 1.23/\omega_0$ at the temperature of the relaxation maximum, if only hydrogen–hydrogen interaction is taken into account. The Γ_1 data measured on $C^{\text{nano}}H_{0.96}$ at $\omega_0/2\pi = 67.7$ MHz show a maximum at about 390 K (cf. Fig. 2(a)), indicating a rather high hydrogen diffusivity already at this temperature. In the other samples with smaller hydrogen content the maxima in Γ_1 are observed at even lower temperatures, namely at 365 K for $x = 0.31$ and at 320 K for $x = 0.24$, indicating an even higher hydrogen mobility. The samples with a smaller hydrogen content are obtained by shorter milling times or by using balls of a smaller mass in the milling process. Such low-concentration samples reveal also fewer defective structures with carbon dangling bonds as suitable trapping sites for hydrogen [4]. This explains quite naturally the somewhat higher hydrogen mobility in the low-concentration $C^{\text{nano}}H_x$ samples. Another interesting feature of the present Γ_1 data is that the relaxation strength seems to be almost the same for all samples, independent of the total hydrogen content. Such a behaviour is expected if each of the hydrogen atoms that contribute to the Γ_1 data has the same number of neighbouring hydrogen atoms at a given distance.

In principle, it can not be excluded that magnetic

impurities, such as elemental iron, are introduced into the samples during the ball-milling procedure. Magnetic impurities may cause a pronounced increase in the relaxation rate [6]. However, about the same maximum relaxation rates, $T_1^{\text{max}} \approx 20 \text{ s}^{-1}$, have been measured in $\text{C}^{\text{nano}}\text{H}_{0.96}$ and $\text{C}^{\text{nano}}\text{H}_{0.24}$. Both samples were prepared using steel vials and balls but with very different milling times. If magnetic impurities are introduced during the milling, the amount should increase with the milling time. Moreover, in the $\text{C}^{\text{nano}}\text{H}_{0.31}$ sample obtained by using agate vials and balls, which should contain less magnetic impurities, a slightly higher maximum relaxation rate, $T_1^{\text{max}} \approx 25 \text{ s}^{-1}$, was observed. From these results we may conclude that, at least in this temperature range, the T_1 data are not strongly affected by magnetic impurities.

In the present NMR studies, a temperature of about 430 K was not exceeded. After the first T_1 data were taken from room temperature to 430 K, further T_1 measurements were performed starting at 430 K down to about 145 K. This second set of T_1 data is shown by the full triangles in Fig. 3. For comparison, the fitting curves of Fig. 2 are also included as solid lines. In the case of $\text{C}^{\text{nano}}\text{H}_{0.96}$, the new measurements are in good agreement with the first T_1 data in their common temperature range (cf. Fig. 2(a)). For the low-concentration samples, on the other hand, these new T_1 data measured from high to low temperatures deviate from the data of the first measurements. However, further T_1 measurements are completely reproducible for all three samples. This is evident from the open triangles in Fig. 3, which represent a third set of T_1 data taken again on warming the samples.

These results remain to be understood, although we suspect that a change in the type of sites occupied by hydrogen in the $\text{C}^{\text{nano}}\text{H}_x$ systems is involved, which occurs if the sample temperature is increased for a certain time to about 400–430 K. We would like to emphasize that 430 K is well below both the temperature of hydrogen desorption and the temperature of recrystallization [4]. Nevertheless, it cannot be excluded that slight changes in the microstructure of the $\text{C}^{\text{nano}}\text{H}_x$ system occur already at this temperature. Even if there is no detectable change in the nanostructure of the graphite itself, some hydrogen atoms may be detrapped at about 400–430 K and subsequently occupy sites with different site energies in the graphite interlayers. The occupation of different sites may result in different energy barriers between neighbouring sites and thus in a distribution of activation energies for hydrogen diffusion. The effects of a distribution of activation energies are to reduce the maximum rate, to broaden the width of the relaxation peak, and to cause the peak to become asymmetric [6]. These features have actually been seen in the case of the low-concentration samples $\text{C}^{\text{nano}}\text{H}_{0.31}$ and $\text{C}^{\text{nano}}\text{H}_{0.24}$ but not in $\text{C}^{\text{nano}}\text{H}_{0.96}$ (cf. Fig. 3). This may indicate that the number of hydrogen atoms being detrapped between 400 and 430 K is a substantial fraction of all hydrogen atoms in the low-concentration

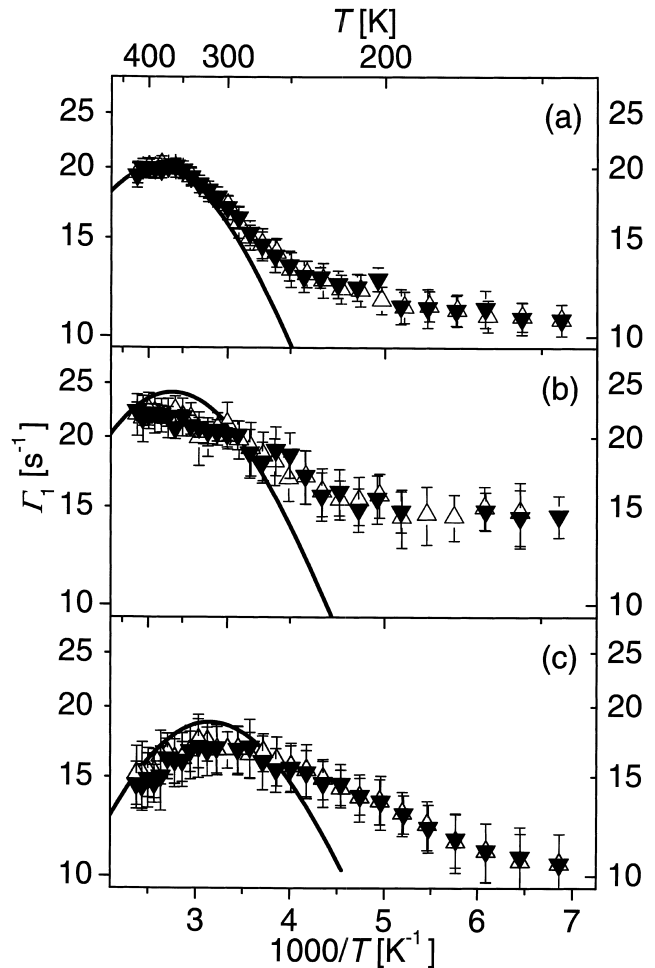


Fig. 3. A second and third set of T_1 data of hydrogen in $\text{C}^{\text{nano}}\text{H}_x$ (a) $x = 0.96$, (b) $x = 0.31$, and (c) $x = 0.24$. The full triangles are data taken from high to low temperatures and the open triangles are data taken subsequently from low to high temperatures. The solid lines are the fit curves of Fig. 2.

samples, whereas it is a negligible fraction in the high-concentration sample $\text{C}^{\text{nano}}\text{H}_{0.96}$. If the shape of the T_1 curves measured on $\text{C}^{\text{nano}}\text{H}_{0.31}$ and $\text{C}^{\text{nano}}\text{H}_{0.24}$ is really due to a distribution of the activation energies, this must also reduce the frequency dependence on the low-temperature side of the relaxation peak. So far, however, we have not measured T_1 at different frequencies and a final conclusion is therefore not yet possible.

Below about 200 K, the T_1 data show a very weak temperature dependence and are most likely not related to hydrogen motion. In this temperature range, the relaxation rate is expected to be dominated by the interaction with the conduction electrons and, possibly, by the presence of strong magnetic moments. It is interesting to note that over the entire temperature range T_1 is higher in the sample prepared by using agate vials and balls than in the two other samples. This result is quite surprising because a sample prepared by mechanical milling with agate vials

and balls should contain a lower level of magnetic impurities.

To further analyse the structure of $C^{\text{nano}}H_x$ and the diffusion mechanisms of hydrogen in these systems, NMR measurements at different NMR frequencies and over more extended temperature ranges are required. The frequency dependence of T_1 has to be studied in order to decide whether a distribution of activation energies exists. A simultaneous analysis of the temperature and frequency dependence of T_1 provides information on the average activation energy and, if there is a distribution, on the distribution width. T_1 measurements at lower temperatures help to determine the contribution due to the conduction electrons and also to separate any contribution due to magnetic impurities. Such measurements are currently being performed in our group.

4. Summary

Nanostructured hydrogen–graphite-systems, $C^{\text{nano}}H_x$, were obtained by mechanical milling of graphite under hydrogen atmosphere. Preliminary nuclear magnetic resonance (NMR) measurements on $C^{\text{nano}}H_x$ ($x = 0.24, 0.31, 0.96$) were performed to study the local environment and the mobility of hydrogen. The NMR spectrum of $C^{\text{nano}}H_{0.96}$ is well represented by the sum of a Lorentzian and a Gaussian line, indicating two types of hydrogen coordinations. These two components may be ascribed to hydrogen in graphite interlayers and hydrogen chemisorbed at dangling bonds. Information on the hydrogen hopping frequencies is provided by the spin–lattice relaxation rate T_1 . The temperature dependence of the T_1 data yields high hydrogen diffusivities with low activation

energies of about $E_a \approx 0.1$ eV. A thermal treatment of the samples at about 430 K affects the T_1 data measured on the $C^{\text{nano}}H_x$ samples with low hydrogen content ($x \leq 0.31$). 430 K is well below both the hydrogen desorption and the recrystallization temperature but nevertheless the microstructure of $C^{\text{nano}}H_x$ seems to change slightly at this temperature. The T_1 data suggest that this change causes a distribution of activation energies for hydrogen motion.

Acknowledgements

This work has been supported by the Deutsche Forschungsgemeinschaft through the graduate college “Modern Methods of Magnetic Resonance in Materials Science” and through Grant No. 446 JAP 113/242/0. The authors are also grateful to Dr. U. Eberle and Dr. M. Schuster for their assistance with the NMR measurements.

References

- [1] S. Orimo, F. Kimmerle, G. Majer, Phys. Rev. B 63 (2001) 94307.
- [2] L. Schlapbach, A. Züttel, Nature 414 (2001) 353.
- [3] S. Orimo, G. Majer, T. Fukunaga, A. Züttel, L. Schlapbach, H. Fujii, Appl. Phys. Lett. 75 (1999) 3093.
- [4] S. Orimo, T. Matsushima, H. Fujii, T. Fukunaga, G. Majer, J. Appl. Phys. 90 (2001) 1545.
- [5] P. Wang, S. Orimo, T. Matsushima, H. Fujii, G. Majer, Appl. Phys. Lett. 80 (2002) 318.
- [6] R.G. Barnes, in: H. Wipf (Ed.), Hydrogen in Metals III, Springer, Berlin, Heidelberg, 1997, p. 93.
- [7] T. Fukunaga, K. Itoh, S. Orimo, M. Aoki, H. Fujii, J. Alloys Comp. 327 (2001) 224.